Granulation Monitoring by Fast Fourier Transform Technique

Atsuo OHIKE,* Kenichi ASHIHARA, and Rinta IBUKI

Technological Development Laboratories, Fujisawa Pharmaceutical Co., Ltd., 2–1–6, Kashima, Yodogawa-ku, Osaka 532–8514, Japan. Received June 28, 1999; accepted August 14, 1999

In the wet granulation process with a high speed mixer, the fast Fourier transform (hereinafter FFT) technique with a personal computer was adopted to perform concurrent precise analysis of the vibration to monitor the granulation process. In this study, a vibration pattern was obtained by inserting a probe into the powder layer. The specific wave pattern of the vibration was observed as granulation progressed. The frequency of the wave was equivalent to that of the impeller blades of the high speed mixer. The elemental strength of the wave at the impeller blade frequency (hereinafter ESWF) converted by FFT exhibits a good relationship with the mass median diameter of the granules. It was demonstrated that the wet granulation process can be concurrently monitored and controlled by ESWF.

Key words wet granulation; end-point; monitoring; high speed mixer; fast Fourier transform

For years, many studies on wet granulation have been conducted and reported. Concerning the operating conditions of a granulation liquid, including granulation time[1—4] and granulation equipment,[5,6] many studies have reported the characteristics of the granules as well as of the final products. In the wet granulation process, determination of the end-point of granulation is crucial in obtaining desirable granules in terms of particle size, tablettability, *etc*. Conventionally, however, the end point of granulation has been empirically judged and adjusted by a researcher by changing the amount of binder liquid, since the end-point varies due to batch differences in raw materials and so on. Recently, the optimization of granulation using experimental research methodology, response surface analysis, statistical experimental design,[7—10] and the possibility of scaling-up[11—13] have been also reported.

As for process monitoring, in the case of the high speed mixer, it is difficult to monitor the end-point by visual observation because of the rapidity of the granulation process. More precise and real-time determination of the granulation end-point would be highly beneficial for pharmaceutical manipulation, such as process control, scaling up and so on. Several attempts were made to monitor the granulation process. Granulation monitoring and end-point determination by several methods, *i.e*., torque of the rotor blade,[14,15] power consumption,[16—18] acoustic emission,[19] and electric conductivity,[20,21] have been reported. In the case of the fluid-bed granulation process, a moisture controlling system[22,23] utilizing an infrared moisture sensor, an acoustic emission sensor system[24,25] which monitors the acoustic emissions caused by the fluidization of granules, and an image analysis system[26] to monitor the fluidization condition have been developed and utilized to monitor and control the granulation process. In the case of the high speed mixer, the blade motor torque[27] and the power consumption of the blade motor[28] have been evaluated; Granusys^{TM} by Fukae PowTec, Japan has been available to monitor granulation using blade motor torque. Watano *et al*.[29,30] studied the wave analysis of the power consumption of the blade motor to evaluate the granulation process, in retrospect, after the granulation was completed. However, the accuracy of detecting precise changes in the granules is limited, because measurement of the torque of the blade motor could be affected by machine conditions such as the lubricant oil used, temperature, *etc*.

Regarding the probe method, many publications[31—34] have reported that the method could determine changes in particle size distribution, density, apparent viscosity, *etc*. As a matter of fact, changes in the granules could be potentially detected more precisely by the probe, which is directly inserted into the granule layer, than by the torque of the blade motor. However, these studies focused on measuring the torque of the probe using a conventional torque measuring device rather than by analyzing the vibration of the probe. Consequently, precise analysis of the vibration has not yet been established.

In this study, a novel approach, *e.g*., evaluation of the vibration of the probe using the fast Fourier transform (FFT) technique, was applied to determine the granulation end point, concurrently with the progress of the granulation process. The objectives of this study were to characterize the wave of the vibration of the probe, to convert the wave into element *versus* frequency by the FFT technique, and to evaluate the applicability of the method to a concurrent end-point monitoring system of granulation.

Experimental

Equipment High Speed Mixer: Pharma Matrix PMAT 25 VG (Fielder, UK). Personal computer: model FMV-5233NP/W (Fujitsu Co., Ltd., Japan). FFT software: Mega view (Keyence Co., Japan). DC Strain Amplifier: model 6M71 (San-ei Instruments, Ltd., Japan). Bridge Box: model 5370 (San-ei Co., Ltd., Japan). Strain Gauge: N32-FA-2-120-11-W3 (San-ei Instruments, Ltd., Japan).

The schematic diagram of the apparatus and the measuring system is shown in Fig. 1. A 25 liter scale high speed mixer, Pharma Matrix PMAT 25 VG (Fielder, UK) was used in this experiment. The probe was pre-determined in terms of the shape of the bottom end, width and length of the shaft, and the position in the vessel. Several probe end shapes, such as a sphere, triangular pyramid, and cube were designed and investigated. The sphere shape was selected because it showed superior reproducibility among the shapes tested, due to minimum adhesion of powder onto the end. Also, several positions of the probe ends, such as the inner or outer side of the powder layer, height, *etc*. were tested. As a result, we selected a probe 3.5 mm in width, 170 mm in length and with a sphere-bottomed end, as shown in Fig. 2, which was positioned at 10 mm above the impeller blade and 30 mm inside the vessel wall, to avoid the adhesion of a wet mass on the probe and to pick up the signal efficiently.

The vibration of the probe was detected by a strain gauge attached to the probe and transmitted to the personal computer *via* a DC strain amplifier and an A/D converter. The vibration signal was concurrently converted as the elemental strength *versus* frequency by FFT using the personal computer.

Materials The optimum high speed mixer formulation, determined by Sunada *et al*.[35] was adopted in this study, as shown in Table 1. The charac-

* To whom correspondence should be addressed.

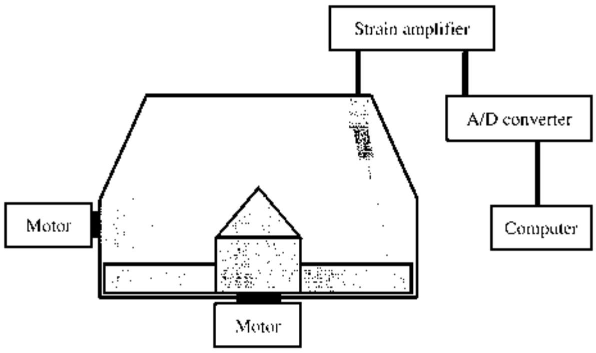

Fig. 1. Auto-Monitoring System for Granulation Process

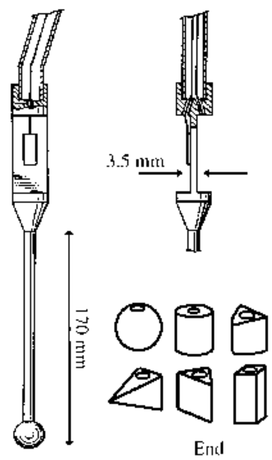

Fig. 2. Design and Dimension of the Probe

Table 1. Experimental Formula as a Batch Size

	Formulation 1 (g)	Formulation 2 (g)
Lactose 100 mesh	3360	—
Lactose 200 mesh	—	3360
Corn starch	1440	1440
Microcrystalline cellulose	200	200
Hydroxypropyl cellulose	150	150
Total	5150	5150

teristics of the materials used are as follows. Lactose 200 mesh (Pharmatose 200M, DMV, Holland): mass median diameter 74 μm, apparent density 458 kg/m^3 and tapped density 798 kg/m^3. Lactose 100 mesh (Pharmatose 100M, DMV, Holland): mass median diameter 121 μm, apparent density 645 kg/m^3 and tapped density 870 kg/m^3. Microcrystalline cellulose (Avicel PH-101, Asahi-Kasei Co., Ltd., Japan): mass median diameter 40 μm, apparent density 321 kg/m^3 and tapped density 440 kg/m^3. Corn starch 120 mesh (Nihon-Shokuhin-Kagaku Co., Ltd., Japan): mass median diameter 15 μm, apparent density 354 kg/m^3 and tapped density 592 kg/m^3. Hydroxypropyl cellulose (HPC-EFP, Shinetsu Chemical, Japan): mass median diameter 102 μm, apparent density 451 kg/m^3 and tapped density 528 kg/m^3. Distilled water was used as a binder.

Method 3360 g of lactose, 1440 g of corn starch, and 200 g of microcrystalline cellulose were mixed with 150 g of hydroxypropyl cellulose in the high speed mixer for 5 min at 300 rpm/1500 rpm (impeller blade/chopper) prior to granulation. Binder liquid was added from the top of the vessel.

In order to evaluate the effect of particle size differences among the raw materials, two grades of lactose particle size were tested, as shown in Table 1. The impeller and chopper were kept at 300 and 1500 rpm, respectively.

At the beginning of the granulation, 900 ml of distilled water was added, followed by an additional 100 ml every 2 min. Each time, at 30 s after the water was added, the mixing operation was stopped and approximately 20 g

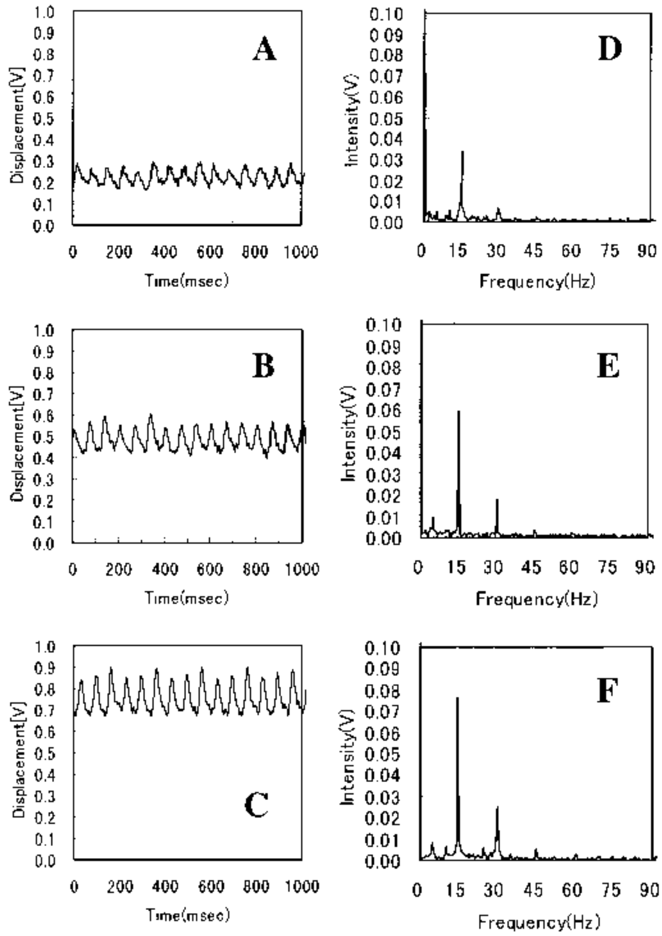

Fig. 3. Typical Original Pattern Change of the Vibration of the Probe during Wet Granulation in a High Speed Mixer and Frequency Conversion Result of Typical Original Pattern of the Vibration of the Probe by FFT Analysis

A, D: at the beginning of the granulation. B, E: in the middle of the granulation. C, F: at the end-point of the granulation.

of the wet mass was removed. The samples were dried for 18 h in a dry heat oven at 40 °C. The characteristics of the granules were evaluated in terms of particle size distribution, shape, apparent specific volume and angle of repose. Particle size distribution was assessed by the sieve method using sieves of 1410, 1000, 850, 500, 355, 250, 180, 150, 106, and 75 μm. The shape was evaluated by observation with a microscope and the aspect ratio of the granules was determined. The apparent specific volume and angle of repose were evaluated using the powder tester made by Hosokawa Micron Corporation.

Results and Discussion

Precise Analysis of the Wave Pattern of Vibration of the Probe during Granulation Process Typical changes in the vibration of the probe during the granulation process are shown in Fig. 3. The vibration strength of the probe, which was indicated by the width of the wave, increased as granulation progressed. In another trial using conventional analog pen recorders, the frequency of the vibration could not be detected accurately, due to the slow response of the analog recorders in comparison with the frequency of the vibration of the probe. However, current digital sampling, whose rate was 1 ms in this study, could detect the precise wave pattern of the vibration. In addition, the FFT technique could conduct a precise analysis of the wave, in terms of frequency. The elemental strength of the waves in Figs. 3-A, B, and C,

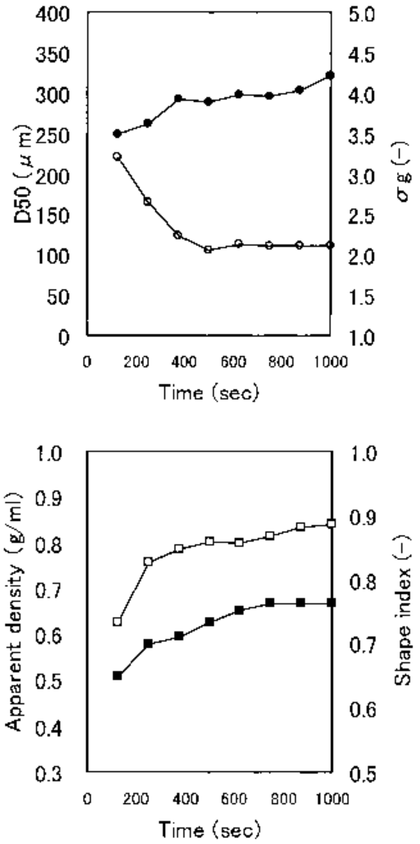

Fig. 4. Relationship between 50% Mean Particle Diameter, Geometric Standard Deviation and Granulation Time during Wet Granulation in a High Speed Mixer and Relationship between Apparent-Density, Shape Index, and Granulation Time during Wet Granulation in a High Speed Mixer.

●, 50% mean particle diameter; ○, geometric standard deviation; ■, apparent-density; □, shape index.

which were obtained by converting the signal into frequency analysis by the FFT technique, were shown in Figs. 3-D, E, and F, respectively.

From the beginning to the end of the granulation, a specific wave pattern of the vibration was observed, and this same wave pattern was observed until the end point of granulation. The width of the probe vibration increased with the progress of granulation, and the displacement of the probe increased as well as indicated by the vertical axes in Figs. 3-A, B, and C. In addition, the frequency analysis by FFT showed that the probe vibration consisted of elements of the specific constant frequencies throughout the granulation. By counting the main peaks in each specific wave pattern, it was clarified that the frequency of the wave fitted with that of the impeller blade of the high speed mixer passing below the probe. For instance, when the impeller with three blades ran at 300 rpm, that is 15 Hz, the observed frequency was 15 Hz. By changing the impeller speed, the same relation was confirmed at other rotation speeds of the impeller. It was also confirmed that the waves were composed of the main elemental strength at the impeller blade frequency with their harmonic frequencies.

These phenomena were interpreted as the impact of the granules upon the probe being made by the blade throughout the granulation process; at the beginning of the granulation process, the finer granules would cause a smaller impact on the probe. With the progress of granulation, as granules developed in size, stronger impacts would thus be made on the probe. The harmonic frequencies were considered to be due to the vibration of the shaft of the probe.

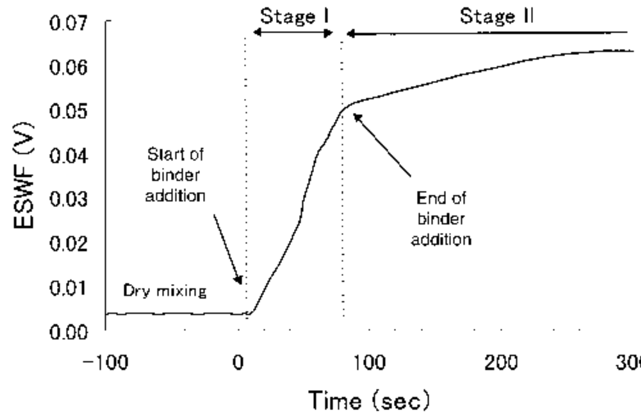

Fig. 5. Typical Pattern Change of ESWF during Wet Granulation in a High Speed Mixer

Granulation Process of the Tested Formulation In order to evaluate the characteristics of the granules of the tested formulation, the mass median diameter, the standard deviation of the particle size distribution, the apparent density, and the aspect ratio of the granules were evaluated in the case of applying 900 ml of binder liquid at a time. The results are shown in Fig. 4. As described in another report,[36] as granulation progressed, the mass median diameter increased, particle size distribution narrowed, and the compaction and spheronization of the granules took place, which were phenomena commonly observed in the conventional high speed granulation process.

The relationship of the mass median diameter of the granules *versus* granulation time was evaluated in different amounts of binder liquid: 900, 1000, 1050, 1100, and 1200 ml, respectively. In all cases, the binder liquid was added all at once at time zero. With the increase in binder liquid at time zero, the mass median diameter of the granules was increased. In addition, in the case of larger amounts of binder liquid, the weight mean diameter increased slightly with granulation time. This indicates that the mass median diameter was affected by the amount of binder liquid, as well as by granulation time, which was characteristic of the tested formulation. As for particle size distribution of the granules, it could be generally said that the particle size distribution of the granules will be determined by the formulation, equipment and operating conditions thereof. In addition, in the case of a high speed mixer, the four processes of 1) distribution of the binder liquid, 2) growth of the granules, 3) formation of secondary granules, and 4) compaction of the secondary granules, occur quickly to form a steady state. Also, the particle size distribution of the granules became steady shortly after applying the additional binder liquid, due to the nature of the formulation tested. Therefore, in this study, the mass median diameter was evaluated in relation to the elemental strength of the wave at the impeller blade frequency (ESWF), because the mass median diameter could be regarded as the most important characteristics in judging the end point of granulation.

Granulation Process and ESWF A typical pattern of ESWF in the case of adding binder liquid all at once is

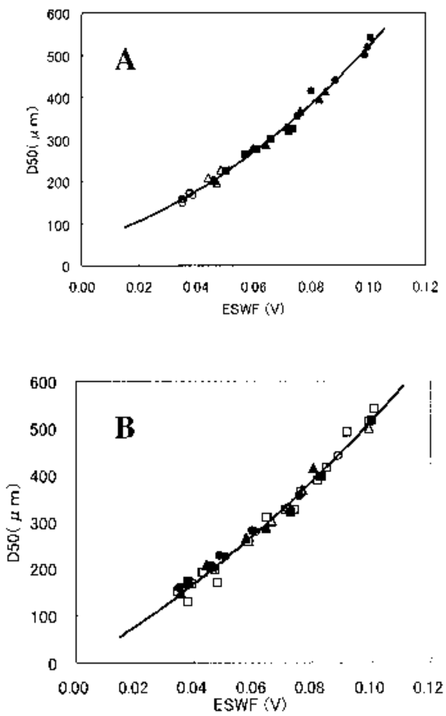

Fig. 6. Relationship between ESWF and 50% Mean Particle Diameter

A: ○, 900 ml; △, 1000 ml; ■, 1050 ml; ▲, 1100 ml; ●, 1200 ml. B: ●, 60 s; ▲, 180 s; ○, 300 s; △, 600 s; ■, 900 s; □, 1000 s.

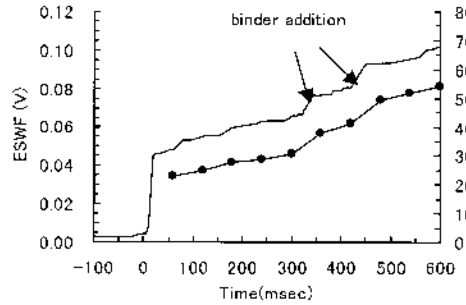

Fig. 7. Effect of Adding Water on Relationship between ESWF, 50% Mean Particle Diameter and Granulation Time

——, ESWF; —●—, D50.

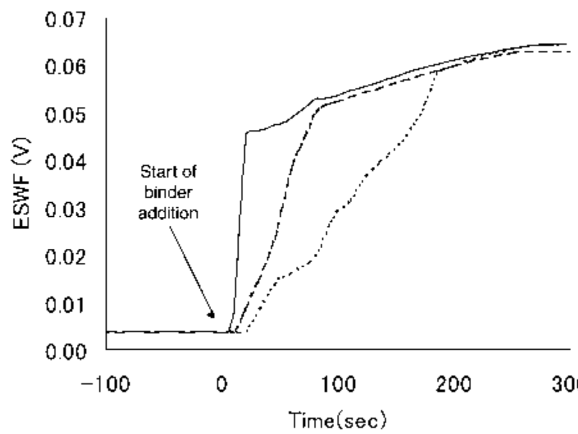

Fig. 8. Effect of Binder Adding Time on Relationship between ESWF and Granulation Time

——, 10 s; – – – –, 90 s; ------, 180 s.

shown in Fig. 5. ESWF showed a two-stage curve as granulation progressed. At the beginning of granulation, when the binder liquid was added, ESWF was increased rapidly, which is called stage 1. Following stage 1, ESWF showed a moderate increase, which is called stage 2. As Terashita *et al.*[37] have reported, stage 1 represents the binder liquid being distributed by the impeller blade and chopper into the powder to create a liquid bridge among fine particles, which causes agglomerates. Stage 2 represents these created agglomerates being compacted to create secondary spherical agglomerates.

In order to evaluate the change in ESWF during the granulation process, 5 different amounts of binder liquids, 900, 1000, 1050, 1100, and 1200 ml, were added to the batches at a time, respectively. As granulation time proceeded, the mass median diameter of each batch increased. In addition, the mass median diameter among the batches of different amounts of binder liquid differed. Nevertheless, the ESWF and the mass median diameter showed a good proportional relationship among the batches, regardless of quantitative differences in the binder liquid, as shown in Fig. 6A. Further, the effect of granulation time on ESWF was also evaluated. Various sampling times were adopted, at 60, 180, 300, 600, 900, and 1000 s, in the different amounts of binder liquid tested. Regardless of the differences in sampling times, ESWF and the mass median diameter of the granules also showed a good proportional relationship, as shown in Fig. 6B. Therefore, it was demonstrated that the ESWF and the mass median diameter of the granules showed a good proportional relationship, regardless of granulation time or the amount of binder liquid.

Effect of binder liquid The impact of additional binder liquid on ESWF during the granulation process was evaluated. The result is shown in Fig. 7. One hundred ml of additional binder liquid was added two times, at 300 and 400 s. Due to the additional binder liquid, the weight mean diameter increased together with ESWF. Although the ESWF showed a rapid increase just after applying the additional binder liquid, this phase was considered to represent the distribution of the binder liquid inside the granules, which was previously defined as stage 1 in this study.

The effect of the liquid flow time on ESWF was also evaluated. As shown in Fig. 8, the supply period was changed to 10, 90 and 180 s. With the increase in supply period, the corresponding period of stage 1 was prolonged, however, stage 2 remained constant. Characteristics of the granules were investigated and are shown in Table 2. Regardless of the binder supply period, ranging from 10 to 180 s, the mass median diameter of the granules and the ESWF thereof exhibited constant values, respectively.

The effect of the particle size of the raw material was evaluated. As a larger raw material, lactose 100 mesh (mass median diameter 121 μm) was replaced with lactose 200 mesh (mass median diameter 74 μm). The granulation results are shown in Fig. 9A. As anticipated, the mass median diameter of the granules was affected by the particle size of lactose. Namely, a larger weight mean diameter of granules was obtained using lactose 100 mesh, even though the amount of binder liquid remained constant. Further, as shown in Fig. 9B, the relationship between the ESWF and the mass median diameter fitted a single proportional curve, regardless of batch differences in raw materials.

Table 2. Physical Properties of Granule in Various Granulating Conditions

No.	Amount of purified water (ml)	Liquid application time (s)	Kneading time (s)	ESWF (V)	Particle size distribution		Apparent density		Angle of repose (°)
					D50 (μm)	σg	Lost (ml/g)	Tapped (ml/g)	
1	1100	10	300	0.066	305	1.95	2.07	1.68	40
2	1100	90	300	0.063	283	1.74	2.05	1.65	39
3	1100	180	300	0.064	297	1.58	2.05	1.65	40
4	1050	10	600	0.066	300	1.92	2.45	1.5	38

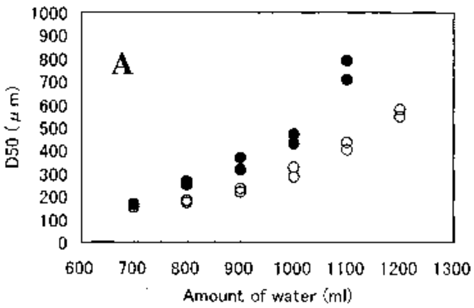

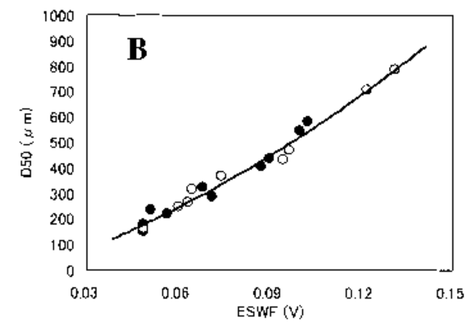

Fig. 9. A: Effect of the Particle Size Difference of Raw Material on the Relationship between the Amount of Water and 50% Mean Particle Diameter

The amount of water is shown as a cumulative percent based on the weight of granulating material.

B: Effect of the Particle Size Difference of Raw Material on the Relationship between ESWF and 50% Mean Particle Diameter

○, small particle size, lactose 200 mesh; ●, large particle size, lactose 100 mesh.

Conclusion

This study demonstrated that with the current digital sampling device, using the FFT technique, the vibration of the probe, which was directly inserted into the powder layer of a high speed mixer, could be analyzed accurately and concurrently with the granulation process. The vibration of the probe was composed of the identical frequency of the blade and the harmonics thereof. ESWF converted by FFT has a good relationship with the mass median diameter of the granules, regardless of the particle size of the starting raw materials or the method of adding binder liquid. Even if the granulation condition is changed, ESWF showed a constant relationship with the mass median diameter of the granules. Therefore, it could be concluded that ESWF can not only monitor the granulation process of a high speed mixer but also optimize the determination of the optimum end point of the granulation process, in terms of the mass median diameter of the granules. The authors have evaluated the effectiveness of the system in a pilot scale described in this article and have also confirmed its applicability to a production scale in another study.[38] This methodology has great potential for controlling the process of granulation. This study also demonstrated that the granulation end-point can be automatically determined by concurrently monitoring the EWSF using FFT. These methods are patented.[39]

References and Notes

1) Holm P., Jungersen O., Schafer T., Kristensen H. G., *Pharm. Ind.*, **45**, 806—811 (1983).
2) Holm P., Jungersen O., Schafer T., Kristensen H. G., *Pharm. Ind.*, **46**, 97—101 (1984).
3) Jaegerskou A., Holm P., Schafer T., Kristensen H. G., *Pharm. Ind.*, **46**, 310—314 (1984).
4) Klistensen H. G., Holm P., Jaegerskou A., Schafer T., *Pharm. Ind.*, **46**, 763—767 (1984).
5) Schafer T., Bak H. H., Jaegerskou A., Kristensen A., Svensson J. R., Holm P., Klistensen H. G., *Pharm. Ind.*, **48**, 1083—1089 (1986).
6) Schafer T., Bak H. H., Jaegerskou A., Kristensen A., Svensson J. R., Holm P., Klistensen H.G., *Pharm. Ind.*, **49**, 297—304 (1987).
7) Vojnovic D., Moneghini M., Rubessa F., *Drug Dev. Ind. Pharm.*, **20**, 1035—1047 (1994).
8) Shirakura O., Yamada M., Hashimoto M., Ishimaru S., Takayama K., Nagai T., *Drug Dev. Ind. Pharm.*, **17**, 471—483 (1991).
9) Aoki S., Okamoto A., Nemoto M., Yoshida T., Danjo K., Sunada H., Otsuka A., *Yakuzaigaku*, **53**, 194—199 (1993).
10) Miyamoto Y., Ryu A., Sugawara S., Miyajima M., Matsui M., Takayama K., Nagai T., *Chem. Pharm. Bull.*, **46**, 1432—1437 (1998).
11) Wehrle P., Nobelis Ph., Cuine A., Stamm A., *Drug Dev. Ind. Pharm.*, **19**, 1983—1997 (1993).
12) Landin M., York P., Cliff M. J., Rowe R. C., Wigmore A., *Int. J. Pharmaceut.*, **133**, 127—131 (1996).
13) Ogawa S., Kamijima T., Miyamoto Y., Miyajima M., Sato H., Takayama K., Nagai T., *J. Pharm. Sci.*, **83**, 439—443 (1994).
14) Lindberg N. O., Leander L., Wenngren L., Helgesen H., Reenstierna B., *Acta. Pharm. Suec.*, **11**, 603—620 (1974).
15) Achanta A. S., Adusumulli P. S., James K. W., *Drug Dev. Ind. Pharm.*, **23**, 539—546 (1997).
16) Holm P., Schaefer T., Kristensen H. G., *Powder Technol.*, **43**, 213—223 (1985).
17) Holm P., Schaefer T., Kristensen H. G., *Powder Technol.*, **43**, 225—233 (1985).
18) Timko R. J., Barrett J. S., Mchugh P. A., Chen S. T., Rosenberg H. A., *Drug Dev. Ind. Pharm.*, **13**, 405—435 (1987).
19) Titley P. C., *J. Pharm. Pharmacol.*, **35**, Suppl. 111, 109P (1983).
20) Fry W. C., Wu P. P., Stagner W. C., Wichman K. C., N. R. Anderson, *Pharm. Tech.*, **11**, 30—42 (1987).
21) Spring M. S., *Drug Dev. Ind. Pharm.*, **9**, 1507—1512 (1983).
22) Watano S., Sato Y., Miyanami K., *J. Chem. Eng. Jpn.*, **28**, 282—287 (1995).
23) Watano S., Sato Y., Miyanami K., *Advanced Powder Technol.*, **6**, 191—199 (1995).
24) Tsujimoto H., Yokoyama T., Sekiguchi I., *Kagaku Kougaku*, **23**, 353—361 (1997).
25) Hidaka J., *Pharm. Tech. Jpn.*, **9**, 19—32 (1993).
26) Ito Y., *Funtai to Kogyo*, **27**, 27—37 (1995).
27) Cliff M. J., *Pharm. Technol. Int.*, **2**, 19—29 (1990).

28) Terashita K., Yasumoto M., Miyanami K., Ohike A., *Yakugaku Zasshi*, **106**, 930—938 (1986).
29) Watano S., Terashita K., Miyanami K., *Chem. Pharm. Bull*., **40**, 269—271 (1992).
30) Watano S., Tanaka T., Miyanami K., *Advanced Powder Technol*., **2**, 91—102 (1995).
31) Kav D., Record P. C., *Manuf. Chem. and Aerosol News*, **48**, 45—46 (1978).
32) Record P. C., *Manuf. Chem. and Arerosol News*, **50**, 65—68 (1979).
33) Staniforth J. N., Walker S., Flanders P., *Int. J. Pharmaceut*., **31**, 277—280 (1986).
34) Staniforth J. N., Quincey S. M., *Int. J. Pharmaceut.*, **32**, 177—185 (1986).
35) Sunada H., *Pharm. Tech. Jpn*., **5**, 299—304 (1989).
36) Terashita K., Kato M., Ohike A., Miyanami K., *Chem. Pharm. Bull*., **38**, 1977—1982 (1990).
37) Terashita K., Ohike A., Kato M., Miyanami K., *Yakugaku Zasshi*, **107**, 377—383 (1987).
38) Not published.
39) Japan. Patent 1975810, 2082019.